Journal of Science and Engineering Technology, Vol. 12, No. 2, pp. 13-23 (2016)

Performance Analysis of Time-Reversal Space Division Multiple Access System

WEI-CHIANG WU
Department of Electrical Engineering, Da-Yeh University
No.168, University Rd., Dacun, Changhua 51591, Taiwan, R.O.C.
wcwm53@mail.dyu.edu.tw

ABSTRACT

In this paper, we propose a time-reversal (TR) downlink space division multiple access communication system. The TR scheme shifts the signal processing needs from the receiver at the radio terminal (RT) to the transmitter at the base station or fixed access point (AP), where power and computational resources are plentiful. We developed two prefiltering schemes: the impulse response of the first prefilter is a time-reversed conjugation of the channel impulse response between the AP and relevant RT. The benefit is spatial and temporal focusing, which collects energy at the sampling instant. The second prefilter meets the zero-forcing criterion such that multiuser interference is completely eliminated at the sampling instants of the relevant RT receiver. Furthermore, we compare the proposed scheme to a downlink direct sequence code division multiple access (DS/CDMA) system that is widely applied in 3G networks. Analytical and simulation results confirm that the superior features of the proposed scheme over the DS/CDMA system lie in the lower complexity, higher throughput, greater flexibility, and practicality.

***Key Words*: Prefilter, Space Division Multiple Access (SDMA), Time reversal (TR), Matched filter (MF), Zero-forcing (ZF), Multiuser interference (MUI).

時間反轉空間分割多工系統的性能分析

武維疆
大葉大學電機工程學系
彰化縣大村鄉學府路 168 號
wcwm53@mail.dyu.edu.tw

摘　要

本文提出了一個下鍊時間反轉空間分割多工系統，時間反轉的架構將複雜的信號處理由行動用戶端移至基地台，我們提出了兩個前置濾波器架構：第一個前置濾波器的脈衝響應為基地台與用戶端之通道脈衝響應時間反轉，其優點為在取樣點空間與時間能量的集中；第二個前置濾波器滿足零強迫的條件，因此多用戶干擾可完全移除。此外，我們比較了直序分碼多工系統，理論與模擬結果證實了本文提出的架構具有低複雜度、高傳輸速率、具有彈性與實用性等優點。

關鍵詞：前置濾波器，空間分割多工，時間反轉，匹配濾波器，零強迫，多用戶干擾。

I. INTRODUCTION

The time-reversal (TR), which is a prefiltering scheme, has been well-studied in wireless communication systems [5] for its full use of multi-path propagation and low-complexity of channel estimation. It has also been applied in underwater acoustic [2] and ultra-wideband (UWB) communication system [6~9, 12, 15]. Recently, it has been shown that TR signal transmission is an ideal paradigm for green wireless communications because of its inherent nature to fully harvest energy from the surrounding environment [11]. A general prefiltering communication system involves two stages: channel estimation and data transmission stages. In the first stage, each end user emits a delta-like pilot pulse that propagates to the basestation or fixed access point (AP) through a richly scattering medium. Then the AP record the multi-path channel impulse response (CIR) that is unique for each user as long as their physical locations are different. Data transmission occurs in the second stage, where AP utilizes the location-specific spatial signatures to remove multiuser interference (MUI) to the intended radio terminal (RT). Attractive features of TR signal processing include:

A. It makes full use of the energy from surrounding environment by exploiting the multi-path propagation: it can create space and time focalization at a specific point where signals are coherently added.
B. Channel estimation in dense multi-path environment is generally a difficult task. The TR technique shifts the sophisticated channel estimation burden from the receivers of RT to the AP.
C. Timing acquisition (synchronization) in TR scheme is extremely simplified since the peak is automatically created and aligned of the received signal at specific time slot.

Most past works of TR scheme focus on the issue of single user transmission and detection. The topic of multiuser TR UWB schemes have been analyzed in [7, 8], where user-specific time-hopping (TH) spreading codes and CIR are jointly employed as signatures for each user. In a rich scattering wireless environment, the multi-path reflection profile between the transmitter and intended receiver can be regarded as a location-specific spatial signature that is unique for the intended RT. Toward this end, a time-reversal division multiplexing scheme is proposed in multi-path channels [3] for a multiuser downlink (from AP to RTs) communication system. This paper considers a time-division duplexing (TDD) scheme, in which reciprocity between uplink and downlink channels can be assumed. The downlink transmission is organized in three phases:

A. Each RT sends a pilot signal to its AP.
B. The AP then uses the received pilot signal to estimate the corresponding CIR.
C. The AP exploits the estimated CIRs to design the corresponding prefilter for each intended RT.

We propose two TR schemes, where a bank of prefilters are designed for each user at the transmitter of AP. The first scheme is referred to as time-reversal matched-filter (TRMF), in which the impulse response (IR) is the time-reversed conjugation of the estimated CIR. Therefore, the multi-path channel serves as a matched filter (MF) to the transmitted waveform. Since the TRMF scheme has excellent spatial-temporal focusing capability, the energy of the received signal tends to concentrate on specific time instants. Hence, a peak is automatically formed at the desired RT and at the end of every bit. This enables us to implement a simple RT receiver to extract the energy at these sampling instants where peak occur. The IR of the second scheme is derived to meet the zero-forcing (ZF) criterion such that MUI is completely removed at the sampling instants of the intended RT receiver. We refer it as the time-reversal zero-forcing (TRZF) scheme.

The rationale of the proposed TR space division multiple access (SDMA) [4, 13, 14] is similar to the DS/CDMA technique that is widely applied in 3G. The pseudorandom (PN) sequence in DS/CDMA corresponds to the IR of the prefilter. Nevertheless, the receiver of DS/CDMA system, which includes synchronization, multiuser detection [10], and channel estimation, is much more complicated than the proposed schemes. Furthermore, the information is easily intercepted as long as the generating algorithm of PN sequence is known by the eavesdropper. In this paper, we will compare and evaluate the performance of DS/CDMA and SDMA from various scenarios.

The remainder of this paper is organized as follows. In section II, we formulate the time-reversed signal model and indoor multi-path fading channel models. Section III highlights the rationale of the prefiltering-based transmission and investigates the performance of the TR-based multiuser system. In section IV, we introduce the DS/CDMA scheme for comparison. Simulation results in terms of the signal-to-interference-plus-noise power ratio (SINR) are presented and analyzed in section V. Concluding remarks are finally made in section VI.

Notation: The boldface letters represent vector or matrix. **A**(i, j) denotes the element of ith row and jth column of matrix **A**. **x**(l) denotes the lth element of vector **x**. $[\ ]^T, [\ ]^H$ stand for transpose and complex transpose of a matrix or vector, respectively. We will use $\|\ \|$ for vector norm, and := for "is defined as". "*" indicates the linear convolution operation. $\mathbf{I}_M$ denotes an identity matrix with size M. $\delta(\cdot)$ is the dirac delta function. $\bar{x}$ denotes the complex conjugate of x.

II. SIGNAL AND CHANNEL MODELS

1. Channel model

In this paper, we consider a multi-user downlink network over multi-path fading channel. The CIR of the communication link between the AP and k-th RT is modeled as

$$h_k(t) = \sum_{l=0}^{L} \alpha_{k,l}\delta(t - lT_c)\ ;\ k=1, 2, \ldots, K \qquad (1)$$

where $\alpha_{k,l}$ is the gain of the lth multi-path component (MPC) of the link between AP and k-th RT. T_c denotes the resolvable time. To simplify the analysis, we assume the channel parameters are quasi-static (slowly fading) such that they are essentially constant over the observation interval. Note that in writing (1), we have modeled the multi-path channel as a tapped-delay line with (L+1) taps. $\alpha_{k,l}$ denotes the tap weight of the lth resolvable path. Moreover, we have implicitly assumed that maximum time dispersion (delay spread) is $T_d = LT_c$.

2. Signal model

We denote kth user's ith bit by $d_k\ i$ and assume the bits sequence, $d_k\ i\ _{\substack{k=1,\ldots,K \\ i=\ldots,1,2,\ldots}}$, are *i.i.d.* random variables, which takes on the value ± 1 with equal probability. If T_b is the bit duration and a_k is the amplitude for kth user, then the binary phase shift-keying (BPSK) signal can be modeled as

$$s_k(t) = \sum_{i=-\infty}^{\infty} a_k d_k(i)\delta(t - iT_b)\ ;\ k=1, 2, \ldots, K \qquad (2)$$

In the proposed TR scheme, a set of K prefilters with IR $\{g_k(t)\}_{k=1,\ldots,K}$ are inserted, respectively, between $\{s_k(t)\}_{k=1,\ldots,K}$ and the transmitting antenna in order to pre-equalize the multi-path fading channels and mitigate the MUI. A TR downlink communication system is depicted in Fig. 1. As shown in the figure, the transmitted waveform $x(t)$ is given by

$$x(t) = \sum_{j=1}^{K}\left[s_j(t) * g_j(t)\right] \qquad (3)$$

Let $h_k(t) = \sum_{l=0}^{L} \alpha_{k,l}\delta(t - lT_c)$ denotes the CIR between the AP and the kth RT, where $\alpha_{k,l}$ represents the fading coefficient of the lth path. Hence, the received signal at the kth RT can be formulated as

$$r_k(t) = x(t) * h_k(t) + n_k(t)\ ;\ k=1, \ldots, K \qquad (4)$$

Substituting (3) into (4), we have

$$\begin{aligned} r_k(t) &= \left(\sum_{j=1}^{K} s_j(t) * g_j(t)\right) * h_k(t) + n_k(t) \\ &= \sum_{j=1}^{K} s_j(t) * p_{jk}\ \ t\ + n_k(t) \end{aligned} \qquad (5)$$

where $p_{jk}\ \ t := g_j(t) * h_k(t)$, $n_k(t)$ is assumed to be zero-mean AWGN noise process with variance σ^2. Please note that the bit duration, T_b, which is up to our disposal, is chosen to be equal to the delay spread (maximum dispersion of the CIR), $T_b = T_d = LT_c$. As shown in Fig. 1, at the front end of each mobile receiver, we sample every bit, sign test is then followed to determine the transmitted bit stream.

$$\hat{d}_k(i) = \mathrm{sgn}\left[r_k(iT_b)\right] \qquad (6)$$

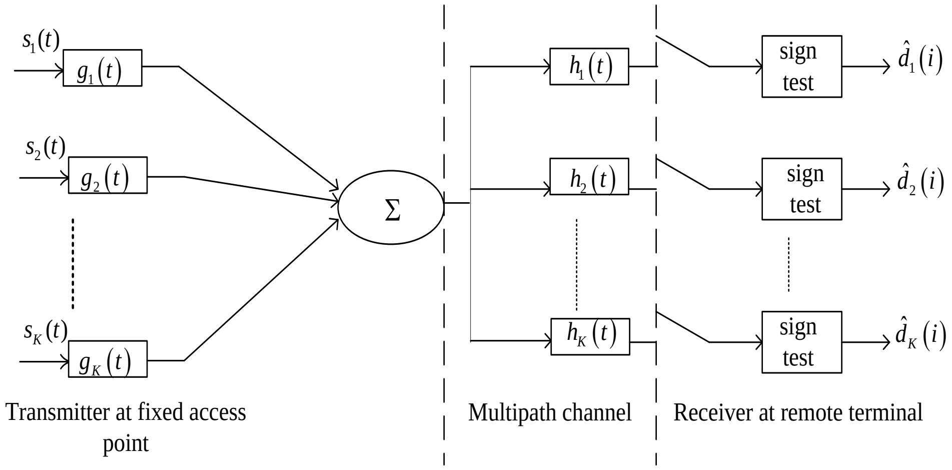

Fig. 1. Structure of a prefiltering-based downlink space division multiple access communication system

where the sign function is defined as

$$\mathrm{sgn}[x] = \begin{cases} 1; x > 0 \\ -1; x < 0 \end{cases}$$

III. DESIGN OF TIME-REVERSAL SDMA SYSTEM

In this paper, we assume a TDD scheme such that channels are reciprocal between the AP and each RT. Thereby, the CIR can be estimated by the AP by receiving sounding pulses (the sounding pulse should be made short enough to approach $\delta(t)$) from each of the RT. Then, a set of prefilters with IR $\{g_k(t)\}_{k=1,\ldots,K}$ are designed based on the estimated CIRs $\{h_k(t)\}_{k=1,\ldots,K}$. Two types of prefilters are proposed in this paper. The first scheme, which is referred to as TRMF, utilizes the time-reversed conjugated CIR as the user-specific signature waveform. Therefore, the multi-path channel serves as a MF to the transmitted waveform. The rationale is equivalent to direct-sequence spread spectrum (DSSS) system, where prefilter and the multi-path channel correspond to the spreader and despreader, respectively. The second scheme, which is referred to as TRZF, fully utilizes the all the CIRs and the prefilter is designed to meet the ZF criterion such that MUI is completely removed at the sampling instants of the intended RT receiver. It should be noted that the receiver at RT is extremely simple since the signal processing is shifted to AP.

1. TRMF scheme

In TRMF scheme, a set of prefilters with IR $g_k(t) = \eta_k \bar{h}_k(T_d - t); k = 1,\ldots,K$ are placed at AP, where η_k denotes the power normalization factor designated to the kth prefilter so that the transmitter bit energy remains a_k^2. It is worthy to note that η_k not only controls the transmit power at AP but also compensates the channel gain (attenuation) in order that the received signal quality at the desired RT is acceptable. In the considered model, $T_d = LT_c$, thus we may rewrite the IR of the TRMF as

$$g_k(t) = \eta_k \bar{h}_k(T_d - t) = \eta_k \sum_{l=0}^{L} \bar{\alpha}_{k,L-l}\delta(t - lT_c); \quad k = 1,\ldots,K \tag{7}$$

Denoting the discrete-time version of the CIRs $h_k(t) = \sum_{l=0}^{L} \alpha_{k,l}\delta(t - lT_c)$ as a $(L+1)$ vector $\mathbf{h}_k := \begin{bmatrix} \alpha_{k,0} & \alpha_{k,1} & \cdots & \alpha_{k,L} \end{bmatrix}^T$, it is easy to deduce that η_k should be chosen as

$$\eta_k = \frac{1}{\sqrt{\sum_{l=0}^{L} \left|\alpha_{k,L-l}\right|^2}} = \frac{1}{\|\mathbf{h}_k\|}; \ k=1, 2, \ldots, K \tag{8}$$

Substituting (8) into (5), the signal received at the kth RT is

$$r_k(t)=\sum_{j=1}^{K} s_j\ \ t\ *\ \eta_j \bar{h}_j(T_d-t)*h_k(t)\ \ +n_k(t) \tag{9}$$

As depicted in (9), the multi-path channel forms a matched filter to the transmitted waveform $g_k\left(t\right)$ due to channel reciprocity. Upon denoting the auto-correlation function of $h_k(t)$ as $R_{k,k}(t) \coloneqq \bar{h}_k(T_d-t)*h_k(t)$, the cross-correlation function between $h_k(t)$ and $h_j(t)\ \ k\neq j$ as $R_{j,k}(t) \coloneqq \bar{h}_j(T_d-t)*h_k(t)$, we may rewrite (9) as

$$\begin{aligned} r_k(t) &= \eta_k s_k(t) * R_{k,k}(t) + \sum_{\substack{j=1\\ j\neq k}}^{K}\left[\eta_j s_j\ \ t\ * R_{j,k}(t)\right] + n_k(t) \\ &= \sum_{i=-\infty}^{\infty}\eta_k a_k d_k\ \ i\ \ R_{k,k}\ \ t-iT_b\ \ + \\ &\quad \sum_{\substack{j=1\\ j\neq k}}^{K}\sum_{i=-\infty}^{\infty}\eta_j a_j d_j\ \ i\ \ R_{j,k}\ \ t-iT_b\ \ +n_k(t) \end{aligned} \tag{10}$$

where the first term at the right-hand-side of (10) is the desired signal, the second term stands for the MUI. If the desired RT is near the basestation while one or some of the undesired RTs are far from the basestation, e.g., at the cell boundary, then the situation of $\eta_k \ll \eta_j;\ j\neq k$ occurs. This results in large MUI that severely degrades system performance.

Denoting the discrete-time version of the CIR of $\bar{h}_k(T_d-t)=\sum_{l=0}^{L}\bar{\alpha}_{k,L-l}\delta\left(t-lT_c\right)$ as a $\left(L+1\right)$ vector $\tilde{\mathbf{h}}_k \coloneqq \left[\bar{\alpha}_{k,L}\ \ \cdots\ \ \bar{\alpha}_{k,1}\ \ \bar{\alpha}_{k,0}\right]^T$, then the discrete-time counterparts of $R_{k,k}(t)$ and $R_{j,k}(t)$ can be formulated, respectively, as

$$\begin{aligned} \mathbf{R}_{k,k} &= \tilde{\mathbf{h}}_k * \mathbf{h}_k \\ &= \begin{bmatrix} \bar{\alpha}_{k,L} & 0 & \cdots & \cdots & 0 \\ \vdots & \bar{\alpha}_{k,L} & \ddots & \ddots & \vdots \\ \bar{\alpha}_{k,0} & \vdots & \ddots & \ddots & \vdots \\ 0 & \bar{\alpha}_{k,0} & \ddots & \ddots & 0 \\ \vdots & 0 & \ddots & \ddots & \bar{\alpha}_{k,L} \\ \vdots & \vdots & \ddots & \ddots & \vdots \\ 0 & 0 & \cdots & 0 & \bar{\alpha}_{k,0} \end{bmatrix}\mathbf{h}_k = \tilde{\mathbf{H}}_k\mathbf{h}_k \end{aligned} \tag{11}$$

$$\begin{aligned} \mathbf{R}_{j,k} &= \tilde{\mathbf{h}}_j * \mathbf{h}_k \\ &= \begin{bmatrix} \bar{\alpha}_{j,L} & 0 & \cdots & \cdots & 0 \\ \vdots & \bar{\alpha}_{j,L} & \ddots & \ddots & \vdots \\ \bar{\alpha}_{j,0} & \vdots & \ddots & \ddots & \vdots \\ 0 & \bar{\alpha}_{j,0} & \ddots & \ddots & 0 \\ \vdots & 0 & \ddots & \ddots & \bar{\alpha}_{j,L} \\ \vdots & \vdots & \ddots & \ddots & \vdots \\ 0 & 0 & \cdots & 0 & \bar{\alpha}_{j,0} \end{bmatrix}\mathbf{h}_k = \tilde{\mathbf{H}}_j\mathbf{h}_k \end{aligned} \tag{12}$$

where the size of the permutation matrix $\bar{\mathbf{H}}_k$, $\tilde{\mathbf{H}}_j$ is $\left(2L{+}1\right)\times\left(L{+}1\right)$. $\mathbf{R}_{k,k}$ and $\mathbf{R}_{j,k}$ are vectors with size $\left(2L{+}1\right)$. It is evident that the magnitude of $\tilde{\mathbf{h}}_k * \mathbf{h}_k$ will coherently add up at the central ((*L*+1)th) position of $\mathbf{R}_{k,k}$, in which the magnitude of the peak is equal to $\mathbf{R}_{k,k}\left(L+1\right)=\sum_{l=0}^{L}\left|\alpha_{k,l}\right|^2=\left\|\mathbf{h}_k\right\|^2$. On the other hand, the other terms will add up non-coherently. Similarly, we can deduce that $\mathbf{R}_{j,k}\left(L+1\right)=\sum_{l=0}^{L}\bar{\alpha}_{j,l}\alpha_{k,l}=\mathbf{h}_j^H\mathbf{h}_k$. Let $T_b = T_d = LT_c$, therefore, the *i*th sample at the *k*th mobile receiver is

$$\begin{aligned} r_k\ \ iT_b\ \ &= \eta_k a_k d_k\ \ i\ \ \mathbf{R}_{k,k}(L+1) + \\ &\quad \sum_{\substack{j=1\\ j\neq k}}^{K}\eta_j a_j d_j\ \ i\ \ \mathbf{R}_{j,k}(L+1)+n_k(iT_b) \\ &= \eta_k a_k d_k\ \ i\ \ \left\|\mathbf{h}_k\right\|^2 + \sum_{\substack{j=1\\ j\neq k}}^{K}\eta_j a_j d_j\ \ i\ \ \mathbf{h}_j^H\mathbf{h}_k + n_k(iT_b) \end{aligned} \tag{13}$$

It follows that the instantaneous SINR at the output of the *k*th user's sampler can be obtained as

$$\gamma_k^{(TRMF)} = \frac{\left(\mathbf{R}_{k,k}\left(L+1\right)\right)^2 a_k^2\eta_k^2}{\sum_{\substack{j=1\\ j\neq k}}^{K}\eta_j^2 a_j^2\left|\mathbf{R}_{j,k}(L+1)\right|^2+\sigma^2} = \frac{a_k^2\left\|\mathbf{h}_k\right\|^2}{\sum_{\substack{j=1\\ j\neq k}}^{K}\dfrac{a_j^2\left|\mathbf{h}_j^H\mathbf{h}_k\right|^2}{\left\|\mathbf{h}_j\right\|^2}+\sigma^2} \tag{14}$$

2. TRZF scheme

The TRZF scheme aims to design prefilters to completely remove MUI. Define the composite IR of *k*th prefilter and *j*th CIR as $p_{kj}\ \ t\ \coloneqq g_k(t)*h_j(t)$, thus the *k*th prefilter should be designed to satisfy the following ZF criteria:

$$p_{kj}\left(LT_c\right)=\begin{cases}0; j\neq k\\ \eta_k; j=k\end{cases}\quad \forall j,k=1,\ldots,K \tag{15}$$

where LT_c is the delay introduced to accommodate the multi-path effect. As depicted in (15), the aim of designing the kth TRZF prefilter, $g_k(t); k=1,\ldots,K$, is to ensure zero interference to the undesired RT while distortionlessly send the data to the desired RT at the sampling instant. We assume the order of $g_k(t)$ being the same as CIR, $g_k(t)=\sum_{l=0}^{L}\beta_{k,l}\delta(t-lT_c)$, though extension to any order is without conceptual difficulty. Denoting the discrete-time version of $g_k(t)$ as a $(L+1)$ vector $\mathbf{g}_k:=\begin{bmatrix}\beta_{k,0} & \beta_{k,1} & \cdots & \beta_{k,L}\end{bmatrix}^T$, then the discrete-time counterparts of $p_{kj}(t):=g_k(t)*h_j(t)\quad \forall j,k=1,\ldots,K$ can be obtained as

$$\mathbf{p}_{kj}=\begin{bmatrix}\bar{\alpha}_{j,0} & 0 & \cdots & \cdots & 0\\ \vdots & \bar{\alpha}_{j,0} & \ddots & \ddots & \vdots\\ \bar{\alpha}_{j,L} & \vdots & \ddots & \ddots & \vdots\\ 0 & \bar{\alpha}_{j,L} & \ddots & \ddots & 0\\ \vdots & 0 & \ddots & \ddots & \bar{\alpha}_{j,0}\\ \vdots & \vdots & \ddots & \ddots & \vdots\\ 0 & 0 & \cdots & 0 & \bar{\alpha}_{j,L}\end{bmatrix}\begin{bmatrix}\beta_{k,0}\\ \beta_{k,1}\\ \vdots\\ \beta_{k,L}\end{bmatrix} \tag{16}$$

where $\mathbf{p}_{kj}$ is a vector with size $(2L+1)$. Since $p_{kj}\left(LT_c\right)=\mathbf{p}_{kj}\left(L+1\right)$, we may exploit (16) to reexpress (15) as

$$\mathbf{p}_{kj}\left(L+1\right)=\sum_{l=0}^{L}\bar{\alpha}_{j,L-l}\beta_{k,l}=\tilde{\mathbf{h}}_j^H\mathbf{g}_k=\begin{cases}0; j\neq k\\ \eta_k; j=k\end{cases} \tag{17}$$

where $\tilde{\mathbf{h}}_j:=\begin{bmatrix}\alpha_{j,L} & \alpha_{j,L-1} & \cdots & \alpha_{j,0}\end{bmatrix}^T$. Upon defining the $(L+1)$ by K matrix, $\tilde{\mathbf{H}}:=\begin{bmatrix}\tilde{\mathbf{h}}_1 & \tilde{\mathbf{h}}_2 & \cdots & \tilde{\mathbf{h}}_K\end{bmatrix}$, (17) can be rewritten as a compact form

$$\tilde{\mathbf{H}}^H\mathbf{g}_k=\eta_k\mathbf{e}_k \tag{18}$$

where $\mathbf{e}_k$ denotes the kth column vector of $\mathbf{I}_K$. If $K\leq\left(L+1\right)$, which is usually the case in dense multi-path environment, we have infinitely many solutions since (18) is indeed an underdetermined system. The minimum-norm solution can be obtained as

$$\mathbf{g}_k=\eta_k\tilde{\mathbf{H}}\left[\tilde{\mathbf{H}}^H\tilde{\mathbf{H}}\right]^{-1}\mathbf{e}_k;\ k=1,\ \ldots,\ K \tag{19}$$

To guarantee $E_b=a_k^2$, η_k should be chosen such that $\left\|\mathbf{g}_k\right\|=1$. It follows from (19)

$$\begin{aligned}\left\|\mathbf{g}_k\right\|^2&=\eta_k^2\mathbf{e}_k^T\left[\tilde{\mathbf{H}}^H\tilde{\mathbf{H}}\right]^{-1}\mathbf{e}_k\\&=\eta_k^2\left[\tilde{\mathbf{H}}^H\tilde{\mathbf{H}}\right]^{-1}\left(k,k\right)\end{aligned} \tag{20}$$

Hence, η_k can be obtained as

$$\eta_k=\frac{1}{\sqrt{\left[\tilde{\mathbf{H}}^H\tilde{\mathbf{H}}\right]^{-1}\left(k,k\right)}} \tag{21}$$

Therefore, the ith sample at the kth mobile receiver is

$$r_k\left(iT_b\right)=\eta_k a_k d_k(i)+n_k(iT_b) \tag{22}$$

As we compare (22) with (13), it is evident that the MUI term vanishes, nevertheless, the received signal power depends on η_k. The instantaneous SINR at the kth RT can be obtained as

$$\gamma_k^{(TRZF)}=\frac{\eta_k^2a_k^2}{\sigma^2}=\frac{a_k^2}{\sigma^2\left[\tilde{\mathbf{H}}^H\tilde{\mathbf{H}}\right]^{-1}\left(k,k\right)} \tag{23}$$

We may also calculate the bit error rate (BER) at the kth RT as

$$Pe_k^{(TRZF)}=Q\left(\frac{\eta_k a_k}{\sigma}\right)=Q\left(\frac{a_k}{\sigma\sqrt{\left[\tilde{\mathbf{H}}^H\tilde{\mathbf{H}}\right]^{-1}\left(k,k\right)}}\right) \tag{24}$$

where $Q(x) := \frac{1}{\sqrt{2\pi}} \int_x^{\infty} \exp\left(-(\frac{\upsilon^2}{2})\right) d\upsilon$ is a monotonically decreasing function with respect to x.

IV. DIRECT-SEQUENCE SPREAD SPECTRUM (DSSS) TRANSMISSION

A general DS/CDMA communication structure is shown in Fig. 2, where the original BPSK data stream is spread by user-specific pulse-shaping filters $\{c_k(t)\}_{k=1,\ldots,K}$.

At the receiving end of kth RT, the received signal can be obtained as

$$
\begin{aligned}
r_k(t) &= x(t) * h_k(t) + n_k(t) \\
&= \sum_i \sum_{j=1}^{K} a_j d_j \ i \ c_j \ t - iT_b \ * h_k(t) + n_k(t) \\
&= \sum_{j=1}^{K} a_j \sum_i d_j \ i \ \sum_{l=0}^{L} \alpha_{k,l} c_j \ t - iT_b - lT_c \ + n_k(t) \\
&= \sum_{j=1}^{K} a_j \sum_i d_j \ i \ \tilde{c}_j \ t - iT_b \ + n_k(t)
\end{aligned} \tag{25}
$$

where $\tilde{c}_j(t) = c_j(t) * h_k(t); j,k = 1,\ldots,K$ represents the effective signature waveform seen by the kth RT. Note that to avoid the presence of intersymbol interference (ISI), we assume a guard period (pending zeros to the end of PN code) of length equal to the delay spread LT_c. At the front end of each RT, chip-matched filtering (CMF) followed by chip-rate sampling, the samples of CMF output within the i-th bit interval at the kth RT can be expressed as

$$
\begin{aligned}
\mathbf{r}_k(i) &= \sum_{k=1}^{K} a_k d_k(i) \tilde{\mathbf{c}}_k + \mathbf{n}_k(i) \\
&= \tilde{\mathbf{C}} \mathbf{A} \mathbf{d}(i) + \mathbf{n}_k(i)
\end{aligned} \tag{26}
$$

where $\tilde{\mathbf{c}}_k$ represents the chip-rate sampled version of the composite waveform. $\tilde{\mathbf{c}}_k$ is vector with size $(N+L)$, where N denotes the length of PN codes. $\tilde{\mathbf{C}} := [\tilde{\mathbf{c}}_1 \quad \tilde{\mathbf{c}}_2 \quad \cdots \quad \tilde{\mathbf{c}}_K]$ is assumed to be full column rank ($(N+L) \geq K$), $\mathbf{A} := diag\{a_1 \quad a_2 \quad \cdots \quad a_K\}$, $\mathbf{d}(i) := [d_1(i) \quad d_2(i) \quad \cdots \quad d_K(i)]^T$. Denoting $\mathbf{c}_{k,l}$ as the chip-rate samples of the received waveform coming from the lth path, thereby each $\mathbf{c}_{k,l}$ represents a delayed version of the original signature vector, $\mathbf{c}_k$. It is evident that $\tilde{\mathbf{c}}_j$ can be expressed as

$$
\tilde{\mathbf{c}}_j = \sum_{l=0}^{L} \alpha_{k,l} \mathbf{c}_{j,l} = \mathbf{C}_j \mathbf{h}_k \ ; j = 1, 2, \ldots, K \tag{27}
$$

where $\mathbf{C}_j := \left[\mathbf{c}_{j,0} \quad \mathbf{c}_{j,1} \quad \cdots \quad \mathbf{c}_{j,L}\right]$. As shown in Fig. 2, linear detection followed by sign test is employed to extract the desired information bits, $d_k \ i$.

$$
\hat{d}_k(i) = \mathrm{sgn}[r_k(i)] = \mathrm{sgn}\left[\mathbf{w}_k^H \mathbf{r}_k(i)\right] \tag{28}
$$

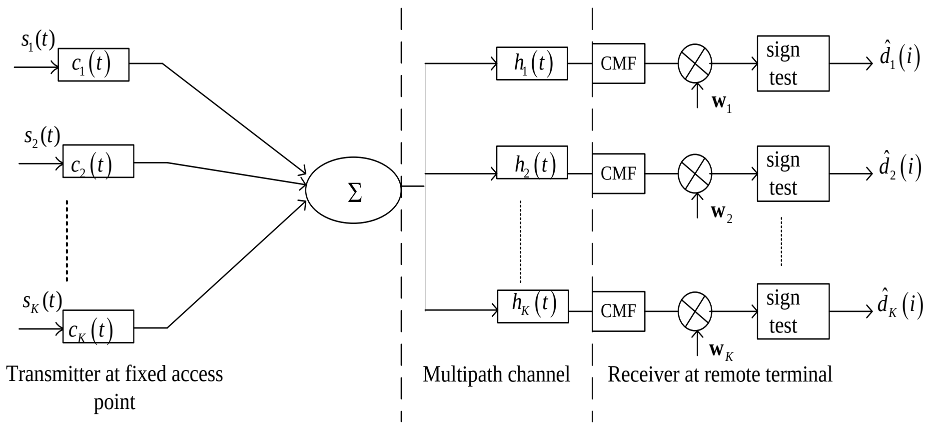

Fig. 2. Structure of a downlink DS/CDMA communication system

Two types of mobile receivers are developed, respectively, in accordance with TRMF and TRZF. The first scheme, which is referred to as MF, utilizes the effective signature of the intended RT to correlate the received signal. The second scheme, which is referred to as ZF, removes all the interference while passes the desired signal distortionlessly.

1. MF scheme

In the MF scheme, $\mathbf{w}_k = \tilde{\mathbf{c}}_k$, substituting into (26), we have

$$r_k(i) = \tilde{\mathbf{c}}_k^H \mathbf{r}_k(i) = a_k d_k(i) \left\|\tilde{\mathbf{c}}_k\right\|^2 + \sum_{\substack{j=1 \\ j\neq k}}^{K} a_j d_j(i) \tilde{\mathbf{c}}_k^H \tilde{\mathbf{c}}_j + \tilde{\mathbf{c}}_k^H \mathbf{n}_k(i) \quad (29)$$

As depicted in (29), the interference power is determined by the near-far problem, crosscorrelation of PN codes and number of RTs. The instantaneous SINR at the *k*th RT can be obtained as

$$\gamma_k^{(MF)} = \frac{a_k^2 \left\|\tilde{\mathbf{c}}_k\right\|^4}{\sum_{\substack{j=1 \\ j\neq k}}^{K} a_j^2 \left|\tilde{\mathbf{c}}_k^H \tilde{\mathbf{c}}_j\right|^2 + \sigma^2 \left\|\tilde{\mathbf{c}}_k\right\|^2} \quad (30)$$

2. ZF scheme

In the ZF scheme, the weight vector at the *k*th RT is designed to meet the following criteria

$$\mathbf{w}_k^H \tilde{\mathbf{c}}_j = \delta_{kj} = \begin{cases} 1; k = j \\ 0; k \neq j \end{cases} \quad (31)$$

It is equivalent to solving the set of linear equations

$$\tilde{\mathbf{C}}^H \mathbf{w}_k = \mathbf{e}_k \quad (32)$$

The minimum-norm solution of (32) can be obtained as

$$\mathbf{w}_k = \tilde{\mathbf{C}} \left[\tilde{\mathbf{C}}^H \tilde{\mathbf{C}}\right]^{-1} \mathbf{e}_k;\ k=1, \ldots, K \quad (33)$$

Substituting (33) into (26), we have

$$r_k(i) = \mathbf{w}_k^H \mathbf{r}_k(i) = a_k d_k(i) + \mathbf{w}_k^H \mathbf{n}_k(i) \quad (34)$$

We can observe from (34) the MUI has been completely removed while the noise power becomes $E\left\{\mathbf{w}_k^H \mathbf{n}_k(i)\right\} = \mathbf{w}_k^H E\left\{\mathbf{n}_k(i)\mathbf{n}_k^H(i)\right\} \mathbf{w}_k = \sigma^2 \left\|\mathbf{w}_k\right\|^2$. Therefore, the instantaneous SINR at the *k*th RT can be obtained as

$$\gamma_k^{(ZF)} = \frac{a_k^2}{\sigma^2 \left\|\mathbf{w}_k\right\|^2} = \frac{a_k^2}{\sigma^2 \left[\tilde{\mathbf{C}}^H \tilde{\mathbf{C}}\right]^{-1}(k,k)} \quad (35)$$

V. PERFORMANCE EVALUATION

In this section, we compare and evaluate the performance of DS/CDMA and TR SDMA from various scenarios. For a fixed *L*, we generate 100 sets of channel parameters, $\left\{\alpha_{k,l}\right\}_{l=0,\ldots,L}$. Each data set is employed for simulation and the result is obtained by taking average of the 1000 independent trials. We employ Walsh codes (Hadamard sequences) in DS/CDMA system as user-specific signature waveforms, which is widely applied in 3G [1]. Note that Walsh codes are the most commonly used orthogonal codes in downlink since it can be easily generated from the Hadamard matrix. Without loss of generality, we assume user 1 is the intended (desired) user hereafter. Unless otherwise mentioned, we set the length of Walsh code (or processing gain) *N*=32, *L*=30, and each user's SNR, which is defined as $\mathrm{SNR}_k := 10\log\left(\frac{a_k}{\sigma}\right)^2$, is set to be 15 dB. Throughout all the simulation examples, MF, ZF, TRMF and TRZF schemes are provided for comparison.

Fig. 3 presents SINR with respect to the number of RTs (denoted by *K*). It is as expected that SINR degrades as *K* increases for both the MF and the TRMF schemes, nevertheless, the performance of the ZF scheme is essentially robust to MUI since the interference is completely removed according to the ZF criterion of (31). Specifically, different from the ZF scheme, the performance of TRZF degrades as *K* increases. This may result from the fact that power normalization factor decreases in accordance with the increase of *K*. Please note also that all the four schemes coincide at *K*=1 (single user). This is due to the fact that the MF-based scheme is optimum in single user case. Fig. 4 shows the performance with respect to the intended user's SNR (denoted by SNR_1), where the number of RTs is set to be 20. As expected, SINR (denoted by γ_1) increases in accordance with SNR_1. The ZF scheme performs better than MF scheme since MUI has been completely removed. To measure the near-far resistance characteristics, we first set all but one of the interferers' (e.g., the *k*th user) amplitudes to be the same as the desired user, $a_1 = a_2 = \cdots = a_{k-1} = a_{k+1} = \cdots a_K$, and define the near-far ratio (NFR) as the power ratio, $\left(\frac{a_k}{a_1}\right)^2$ (in dB). Let $\mathrm{SNR}_1 = 12\mathrm{dB}$, by varying NFR from 0 to 10 dB, the performance of γ_1 is presented in Fig. 5. As we can observe from the figure, both the ZF and TRZF schemes are invariant for the increase of NFR, while γ_1 slowly decays for the MF and TRMF schemes. This demonstrates that both ZF and TRZF schemes are applicable in practical near-far environment. In the final simulation example, we measure γ_1 with respect to the length of CIR (or equivalently, the prefilter length), where we set *K*=20. As shown in Fig. 6, the MF and ZF schemes for DS/CDMA system are insensitive to *L*, whereas the performance of both TRMF and TRZF schemes get better as prefilter length (denoted by *L*) increases. It verifies the fact that in TR scheme, prefilter length corresponds to the degrees of freedom or processing gain which determines the capability of mitigating MUI.

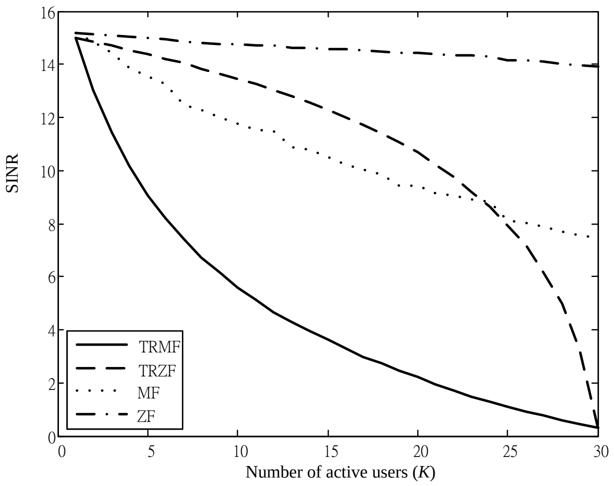

Fig. 3. SINR performance with respect to the number of RTs

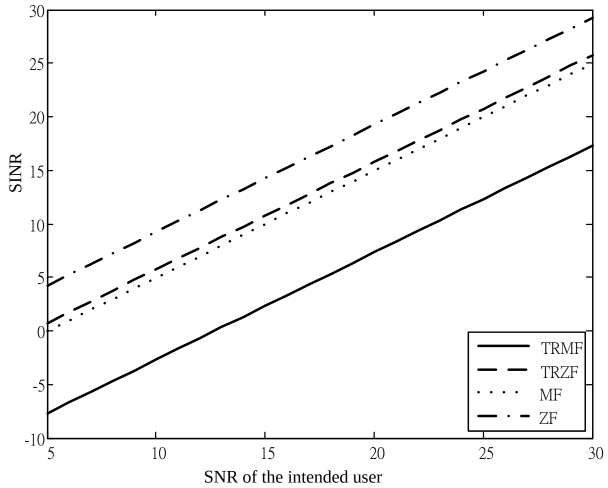

Fig. 4. System performance with respect to the desired user's SNR.

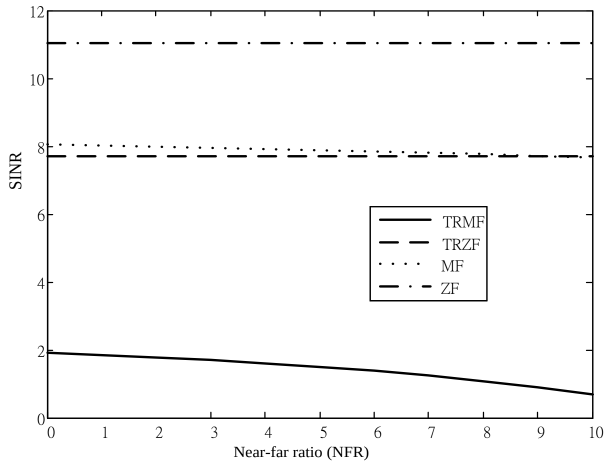

Fig. 5. System performance with respect to near-far ratio (NFR)

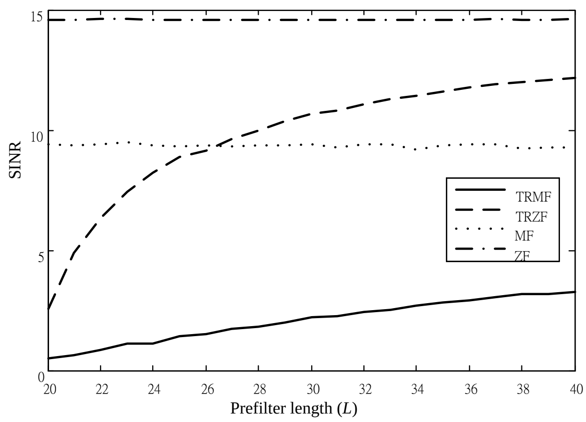

Fig. 6. SINR performance with respect to prefilter length

According to the above results, several remarks can be made:

A. As revealed by the simulation results, the MF and ZF schemes for DS/CDMA system outperforms TRMF and TRZF schemes, respectively. The main reason arises from the fact that DS/CDMA downlink system utilizes Walsh codes as the user-specific signature waveforms. As is well-known, the Walsh codes are the most commonly used orthogonal codes. Nevertheless, the proposed TR SDMA scheme exploits the instantaneous CIRs to generate signature waveforms. An obvious flaw of this scheme is that spatial channels are rarely orthogonal in practice. In what follows, the MUI of the DS/CDMA system is expected to be smaller than the proposed TR SDMA scheme.

B. Though DS/CDMA system outperforms the proposed TR SDMA scheme, nevertheless, channel and timing estimation are difficult to accomplish in RT of DS/CDMA system. Moreover, in richly scattering environment, the inevitable estimation error severely deteriorates system performance in DS/CDMA system with high processing gain.

C. In spite of the channel estimation problem as mentioned above, applying the RAKE receiver for DS/CDMA system in a richly scattering environment is problematic. Consider the state-of-the-art mobile receiver for DS/CDMA system, the number of RAKE fingers is less than 7, which means most of the energies are wasted in extreme multi-path channel. Whereas, the prefiltering technology is able to gather energy from all the paths.

D. From the throughput (bits per second) viewpoint, there are $N+L$ chips within a bit for DS/CDMA system, where L is the guard period prevented from ISI. In prefiltering system, the prefilter length, which corresponds to a bit duration, is only L chips. Therefore, the ratio in terms of throughput is $\frac{N+L}{L}$. In general, $N \gg L$, which indicates that TR system is much more efficient than DS/CDMA system.

E. It is well-known that applying a ZF filter (or equivalently, decorrelating detector) in the receiver to remove MUI will enhance the additive background noise [10]. Moreover, as depicted in (33), to implement the ZF receiver at RT requires the information of all the PN codes $\left\{c_k\left(t\right)\right\}_{k=1,\ldots,K}$ as well as all the CIRs $\left\{h_k\left(t\right)\right\}_{k=1,\ldots,K}$. However, in practical situation, it is difficult for the RT to acquire these information.

F. The power normalization factor η_k dominates system performance of the TRZF scheme, where a decrease of η_k leads to performance degradation. As depicted in (21), several factors determine the value of η_k, e.g., as K increases, η_k decreases as well. We have verified in Fig. 3 that larger K deteriorates system performance of the TRZF scheme.

Ⅵ. CONCLUSIONS

In this paper, two TR SDMA schemes have been proposed and applied in wireless communication system over dense multi-path channel. The benefit of the proposed scheme is that it lessens the burden in signal processing of the RT receiver where an extremely simplified receiver is typically required. The simulation results have demonstrated that the performance of the proposed TR SDMA system is comparable to the DS/CDMA system, nevertheless, it is much more superior to the DS/CDMA system in terms of complexity, throughput, and practicability. The difficulty may arise in applying the prefiltering technique is in fast fading channel. The RT may require to continuously emitting sounding pulses in order that the transmitter of AP has immediately information of CIRs, which leads to decrease of efficiency.

REFERENCES

1. Ali, A. R. M. (2007) *Introduction to CDMA wireless communications*, Elsevier Academic Press, Burlington, MA
2. Blomgren, P., P. Kyritsi, A. Kim and G. Papanicolaou (2008) Spatial focusing and intersymbol interference in multiple-input-single-output time reversal communication systems. *IEEE Journal of Oceanic Engineering*, 33(3), 341-355.
3. Han, F., Y. H. Yang, B. Wang, Y. Wu and K. J. R. Liu (2011) Time-reversal division multiple access in

multi-path channels. IEEE Global Communications Conference (Globecom), Houston.
4. Llcev, S. D. (2011) Space division multiple access (SDMA) applicable for mobile satellite communications. 10th International Conference on Telecommunication in Modern Satellite Cable and Broadcasting Services (TELSIKS), Serbia.
5. Nguyen, H. T., J. B. Andersen, G. F. Pedersen, P. Kyritsi and P. C. F. Eggers (2006) Time reversal in wireless communications: a measurement-based investigation. *IEEE Transactions on Wireless Communications*, 5(8), 2242-2252.
6. Nguyen, H. T., I. Z. Kovacs and P. C. F. Eggers (2006) A time reversal transmission approach for multiuser UWB communications. *IEEE Transactions on Antennas and Propagation*, 54(11), 3216-3224.
7. Qiu, R. C. (2006) A theory of time-reversed impulse multiple-input multiple-output (MIMO) for ultra-wideband (UWB) communications. International Conference on Ultra-wideband, ICUWB'06, Waltham, MA.
8. Qiu, R. C., C. Zhou, J. Q. Zhang and N. Guo (2006) Channel reciprocity and time-reversed propagation for ultra-wideband communications. *IEEE Antenna and Wireless Propagation Letters*, 5(1), 269-273.
9. Strohmer, T., M. Emami, J. Hansen, G. Papanicolaou and A. J. Paulraj (2004) Application of time-reversal with MMSE equalizer to UWB communications. GLOBECOM'04: IEEE Global Telecommunications Conference, Dallas, Texas.
10. Verdu, S. (1998) *Multiuser Detection*, Cambridge University Press.
11. Wang, B., Y. Wu, F. Han, Y. H. Yang and K. J. R. Liu (2011) Green wireless communications: a time-reversal paradigm. *IEEE Journal on Selected Areas in Communications*, 29(8), 1698-1710.
12. Wu, W. C. (2009) Prefiltering-based interference suppression for time-hopping multiuser UWB communications over MISO channel. *EURASIP Journal on Advances in Signal Processing*, Article ID 617298, doi:10.1155/2009/617298, 10 pages.
13. Yin, H. and H. Liu (2002) Performance of space-division multiple-access (SDMA) with scheduling. *IEEE Trans. on Wireless Communications*, 1(4), 611~618.
14. Zhao, M., M. Ma and Y. Yang (2011) Efficient data gathering with mobile collectors and space-division multiple-access techniques in wireless sensor networks. *IEEE Transactions. on Computers*, 60(3), 400~417.
15. Zhou, C., N. Guo and R. C. Qiu (2006) Experimental results on multiple-input single-output (MISO) time reversal for UWB systems in an office environment. Military Communications Conference (MILCOM06), Washington D. C.

收件：**105.01.13** 修正：**105.04.01** 接受：**105.05.06**